Tree Physiology 34, 1018–1029
doi:10.1093/treephys/tpu061

Research paper

Xylan deposition and lignification in the multi-layered cell walls of phloem fibres in *Mallotus japonicus* (Euphorbiaceae)

Kaori Nakagawa, Arata Yoshinaga[1] and Keiji Takabe

Laboratory of Tree Cell Biology, Division of Forest and Biomaterials Science, Graduate School of Agriculture, Kyoto University, Sakyo-ku, Kyoto 606-8502, Japan; [1]Corresponding author (aryosshy@kais.kyoto-u.ac.jp)

Received January 29, 2014; accepted June 26, 2014; published online August 23, 2014; handling Editor Ron Sederoff

Phloem fibres in *Mallotus japonicus* Müll. Arg. were found to have a multi-layered structure that is $S_1+S_2+n(G+L)$, where a non-lignified gelatinous layer (G) and a lignified layer (L) are formed alternately and *n* indicates the number of repetitions of these two layers. The aim of this study was to determine the process of xylan deposition and lignification in the multi-layered cell walls of phloem fibres. The formation process of the multi-layered structure of secondary phloem fibres was examined by light microscopy, ultraviolet microscopy and transmission electron microscopy. The distribution of glucuronoxylan was examined by immunoelectron microscopy. The activity of peroxidase was also determined using metal-enhanced diaminobenzidine substrates. Immunolabelling of glucuronoxylan occurred in lignified cell wall layers, except in the compound middle lamella (CML), i.e., the S_1, S_2 and L layers but not the G layers. Change in immunolabelling density suggests that xylan deposition in these lignified layers occurs appositionally, i.e., xylan is deposited into the lignified layers directly and not by a penetrative mechanism, and deposition does not occur after the layers are fully deposited. Peroxidase activity was found in CML including cell corners during S_2 layer formation, then in developing G layers during G layer formation. Peroxidase activity was also found in the thin L layers that formed recently and was not found in the L layers already present. Xylan labelling was not found in the thin L layers that formed recently but did occur in L layers that developed earlier. Lignification of the S_1 and S_2 layers continued during the formation of the G layers, whereas in the L layers it finished just after deposition of the L layer.

Keywords: gelatinous layer, glucuronoxylan, lignin, peroxidase.

Introduction

In most trees, the secondary phloem contains phloem fibres and/or sclereids. Phloem fibres and sclereids are lignified, whereas other cell types (e.g., sieve cells in gymnosperms, sieve tube members in angiosperms, phloem parenchyma cells and phloem ray parenchyma cells) are not lignified. Phloem fibres are derived from cambial initials, whereas sclereids are derived secondarily from either phloem parenchyma cells or phloem ray parenchyma cells. Phloem fibres and sclereids have thick lignified secondary walls that strengthen the secondary phloem in tree bark. Wood fibres in the xylem are arranged radially in the order of cell differentiation through radial files; hence the process of cell wall formation can be easily investigated through the radial files. In contrast, phloem fibres are usually arranged in the form of tangential bands or small groups in the phloem. Because of their discontinuous arrangement, the lignification process of phloem fibres has not been investigated as thoroughly as that of wood fibres in xylem.

Imagawa and Ishida (1973) examined the seasonal development of secondary phloem in *Kalopanax pictus* (Thunb.) Nakai. They reported that lignification of phloem fibres began at cell corners far from the cambium and then proceeded toward

secondary walls. Nanko et al. (1974) studied the development and differentiation of secondary phloem and the morphological changes occurring after maturation in *Populus euramericana* Guinier by light microscopy, and found that phloem fibres consisted of S_1 and S_2 layers. They also found phloem fibres with three to five layers in a part of a specimen collected from the upper part of an inclined stem. Nanko et al. (1977) then examined the cell wall structure of phloem fibres in the secondary phloem of *P. euramericana* using electron microscopy and found that S_1 layers had a flat S helix whereas S_2 layers had a steep Z helix.

Nanko (1979) examined the cell wall structure of phloem fibres in 38 Japanese tree species belonging to 23 genera. He classified phloem fibres into the following three types according to the structure of the cell wall layers: (i) S_1+S_2 type, (ii) S_1+S_2+G type and (iii) $S_1+S_2+n(G+L)$ type, where *n* indicates the number of repetitions of the thick non-lignified gelatinous layer (G) and the thin lignified layer (L). Further study determined that the third type of phloem fibres in the reaction phloem of *P. euramericana* (Nanko et al. 1982) and *Salix koriyanagi* Kimura might be related to the reaction phenomenon. Recently Nakagawa et al. (2012) investigated the anatomy and lignin distribution of the reaction phloem in several Japanese hardwoods and found that phloem fibres in *Mallotus japonicus* Müll. Arg. were of the $S_1+S_2+n(G+L)$ type and the number of repetitions (*n*) increased on the upper side of an inclined stem. A multi-layered structure was also reported for tension wood fibres in the xylem of tropical hardwoods (Clair et al. 2006, Ruelle et al. 2007). For cells with this multi-layered structure, the synthesis and transportation of monolignols is temporally regulated during the formation of multi-layered cell walls because non-lignified and lignified cell wall layers are formed alternately. Therefore, phloem fibres with a multi-layered structure are of interest when considering monolignol synthesis and transportation. The aim of the present study was to clarify the formation process of multi-layered cell walls in the phloem fibres of *M. japonicus*. We also examined the presence of glucuronoxylan, which is thought to be the host structure of the lignification process (Reis and Vian 2004), as well as the activity of peroxidase, which catalyses the polymerization of monolignols.

Materials and methods

Plant materials

Three- to 5-year-old *M. japonicus* trees, grown at the Kitashirakawa Experimental Station, Field Science Education and Research Center, Kyoto University, Kyoto, Japan (35°N, 136°E), were cut from the beginning of April to the beginning of December. Details of the trees used in the present study are shown in Table 1. Although some trees were slightly tilted, the lower opposite position or side position was selected to avoid the effect of the reaction phenomenon.

Table 1. Trees used in the present study. DBH, diameter at breast height.

No.	Sampling	Height (cm)	DBH (cm)	Tree age (years)
1	8 April 2009	546	2.93	3
2	18 May 2009	570	3.18	5
3	16 June 2009	630	4.14	4
4	2 July 2010	205	1.59	3
5	9 July 2009	400	2.50	5
6	9 Sept. 2009	295	2.55	3
7	29 Oct. 2009	500	4.30	4
8	16 Nov. 2009	460	2.23	4
9	2 Dec. 2008	530	3.50	3
10	18 June 2013	534	3.18	4
11	2 July 2013	630	4.39	5

Light microscopy

Small blocks were cut from the trees with a razor blade, stored in 70% ethanol, and then dehydrated through an ethanol series and embedded in epoxy resin according to the method of Luft (1961). Methyl nadic anhydride is known to be strongly stained by potassium permanganate in electron microscopy and was not used in our method. Dodecenyl succinic anhydride was used as a replacement. Sections of 1 μm thickness were cut from the embedded specimens and stained with 0.5% Azure II–methylene blue aqueous solution containing 0.5% borax ($Na_2B_4O_7 \cdot 10H_2O$) (Richardson et al. 1960) for 3 min on a hot plate at 50 °C, washed with water and dried. Sections were then mounted with Canada balsam and observed under a light microscope (Olympus BX50, Tokyo, Japan) equipped with a digital camera (Olympus DP70, Tokyo, Japan).

Ultraviolet microscopy

Transverse sections (3 μm thick) were prepared from specimens embedded in epoxy resin, mounted on quartz slides with glycerine and covered with quartz coverslips. Ultraviolet (UV) photomicrographs were taken at 280 nm using a microspectrophotometer (UMSP-80, Carl Zeiss, Germany) and recorded with a digital camera (CM-140GE-UV, JAI Corp., Yokohama, Japan) and JAI Control Tool software.

Electron microscopy following staining with potassium permanganate

Ultrathin sections (~0.1 μm thick) were cut from embedded specimens with an ultramicrotome (Reichert-Jung ULTRACUT E, Heidelberg, Germany) equipped with a diamond knife. Sections were mounted on copper grids and stained with 1% potassium permanganate and 0.1% sodium citrate aqueous solution for 30 min at room temperature. They were then washed with water and observed under a transmission electron microscope (TEM, JEM 1220 or JEM 1400, JEOL Ltd, Tokyo, Japan) at 100 kV.

Immunogold labelling of glucuronoxylan

Ultrathin sections were cut from the embedded block and mounted on nickel grids (200 mesh). The sections were floated on a drop

of blocking buffer (1% BSA, 0.1% NaN_3, 0.1% Tween 20 in Tris–hydrochloric acid-buffered saline (TBS)) for 30 min at room temperature. The sections were then floated on a drop of primary antibody for 2 days at 4 °C. To detect glucuronoxylan, LM10 or LM11 rat hybridoma supernatant (PlantProbes, Leeds, UK, McCartney et al. 2005) was diluted in a 1 : 20 ratio with blocking buffer. Following washing three times for 15 min each with drops of blocking buffer, the sections were incubated with goat anti-rat secondary antibody labelled with 10 nm colloidal gold particles (EMGAT10; BB International, Cardiff, UK) diluted in a 1 : 100 ratio with blocking buffer. Finally, the sections were washed six times for 15 min each with drops of blocking buffer and then washed with deionized water. Sections were observed under a TEM (JEM 1400, JEOL Ltd) at 100 kV without post-staining.

Activity staining of peroxidase with metal-enhanced DAB substrate

The activity of peroxidase was detected using a metal-enhanced diaminobenzidine (DAB) substrate kit (Thermo Fisher Scientific Co. Ltd, Yokohama, Japan, Adams 1981). From Trees 10 and 11 collected on 18 June 2013 and 2 July 2013, respectively, transverse sections (60 µm thick) were cut and treated with DAB/metal concentrate diluted in a 1 : 10 ratio with stable peroxide buffer for 30 min at room temperature. After washing with water, sections were put on glass slides, mounted with water and observed under a light microscope. As a negative control, the sections were treated with stable peroxide buffer without DAB/metal concentrate.

To observe peroxidase activity on cell wall layers including very thin L layers at higher resolution, DAB staining followed by osmium tetroxide post-fixation was performed for transmission electron microscopy (Graham and Karnovsky 1966). Small blocks were cut from the specimen collected on 2 July 2010 (Tree 4) using a razor blade and treated with DAB/metal concentrate diluted in a 1 : 10 ratio with stable peroxide buffer for 30 min at room temperature. After washing with phosphate-buffered saline three times for 5 min each, blocks were post-fixed with 1% osmium tetroxide aqueous solution, washed with phosphate buffer, dehydrated through an ethanol series and embedded in epoxy resin as described above. As a negative control, the blocks were treated with stable peroxide buffer without DAB/metal concentrate and then post-fixed with 1% osmium tetroxide and then embedded in epoxy resin. Ultrathin sections were cut from the embedded block and mounted on copper grids. The sections were observed under a TEM (JEM 1400, JEOL Ltd) at 100 kV without post-staining.

Results

Cell wall formation of phloem fibres

The seasonal development of secondary phloem and the process of cell wall formation in phloem fibres are shown in Figure 1. Under the Azure II–methylene blue staining, the non-lignified and lignified cell wall shows purple and blue colour, respectively. At the beginning of April, the cambium had not been reactivated. The first group of sieve tube members and phloem parenchyma cells were differentiated by the middle of May (data not shown). Phloem fibres with very thin secondary walls were differentiated by the middle of June (Figure 1a and d). Secondary wall thickening of phloem fibres progressed throughout the beginning of July (Figure 1b and e). Further thickening of phloem fibres occurred throughout the beginning of September (Figure 1c and f), with cambial activity almost ending by the end of October. Cell wall thickening of phloem fibres had progressed further by the end of October (Figure 1g and j) and by the middle of November (Figure 1h and k), but had almost finished by the beginning of December, with deposition of thick lignified innermost layers (Figure 1i and l). It should be noted that the stages of development were not necessarily the same within the group of phloem fibres. In addition, the number of repetitions (n) of the multi-layered structure $S_1+S_2+n(G+L)$ differed within the group of phloem fibres as reported by Nakagawa et al. (2012). Therefore in the present study, the formation process is discussed according to the stage of development of individual phloem fibres rather than the sampling date.

Lignin distribution and lignification process of different cell wall layers

Figure 2 shows UV and TEM micrographs of transverse sections of almost fully developed phloem fibres. These micrographs clearly show that the compound middle lamella (CML), S_1, S_2 and L layers are lignified, but G layers are not lignified. The lignification process for these lignified layers of phloem fibres was examined using specimens at different stages of formation as shown in Figure 1. G and L layers were numbered from the outside, for example, G_1, G_2, G_3 and L_1, L_2, L_3 (Figure 2b).

Figure 3 shows UV photographs from transverse sections taken at different developmental stages. Lignification started at the cell corner in the middle lamella (arrows in Figure 3a) and then proceeded towards the CML, S_1 and S_2 layers (Figure 3b–d). Because the degree of UV absorption of the S_1 and S_2 layers was increasing during G+L layer deposition (compare Figure 3b with Figure 3a), it can be assumed that lignification of the S_1 and S_2 layers occurred during the formation of the G and L layers. When cell wall formation was completed, strong UV absorption was found in the CML, S_1, S_2 and L layers (Figure 3d).

Figures 3e–g and 4 are TEM micrographs showing transverse ultrathin sections after staining with potassium permanganate at different developmental stages. During the formation of the S_2 layer (Figure 3e), lignification started at the cell corner in the middle lamella, although the degree of staining of the

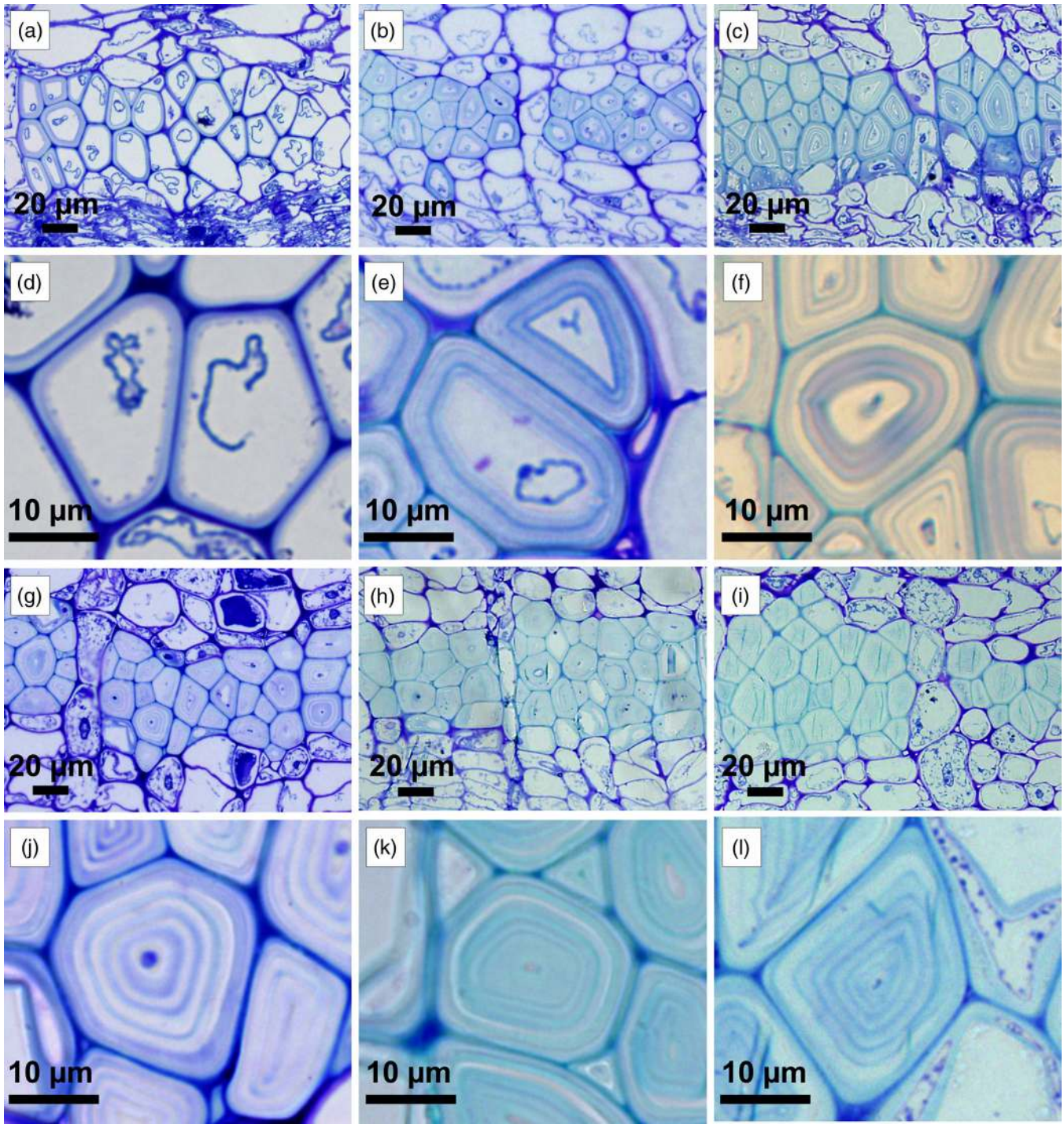

Figure 1. Light micrographs of transverse sections stained with Azure II–methylene blue showing the formation of phloem fibres in *M. japonicus* collected on 16 June 2009 (Tree 3, a and d), 9 July 2009 (Tree 5, b and e), 9 September 2009 (Tree 6, c and f), 29 October 2009 (Tree 7, g and j), 16 November 2009 (Tree 8, h and k) and 2 December 2009 (Tree 9, i and l).

S_1 and S_2 layers and the middle lamella between cell corners was low. When the thin G_1 layer was formed (Figure 3f), the degree of staining in the CML increased, whereas in the S_1 and S_2 layers it did not increase. When the L_1 and G_2 layers were formed inside the G_1 layer (Figure 3g), the degree of staining of the S_1 and S_2 layers increased, suggesting that lignification of these layers progressed during the formation of the G layer. When the very thin third L layer (L_3) was formed inside the third G layer (G_3), the L_3 layer had a much stronger staining than the outer L_1 and L_2 layers and the innermost G layer (G_3), which also had a stronger staining than the outer G_1 and G_2 layers (Figure 4a and b). When the L_3 layer was fully formed,

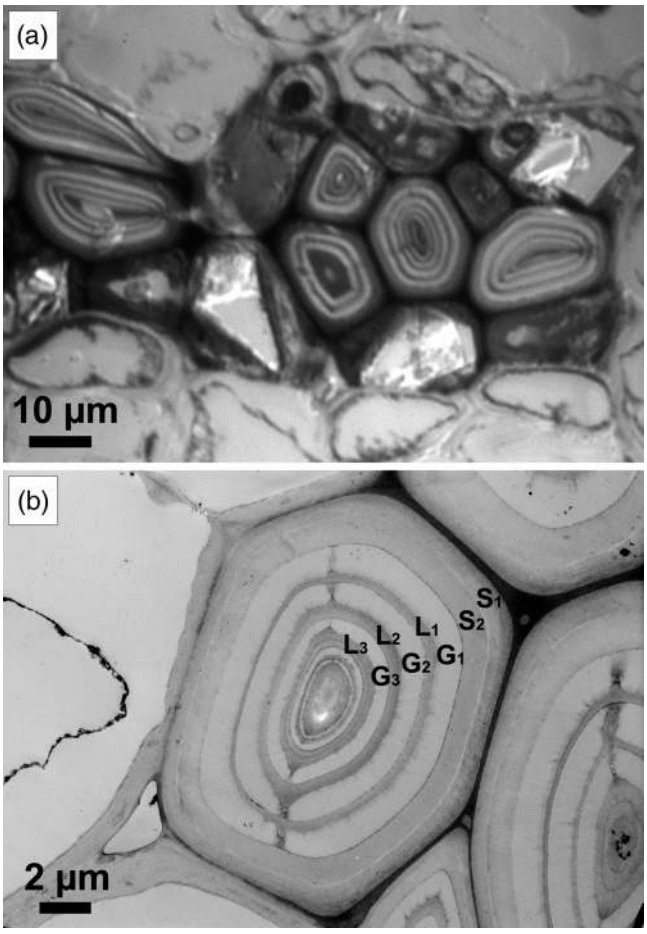

Figure 2. A UV micrograph taken at 280 nm of phloem fibres in *M. japonicus* (Tree 9, a) showing UV absorption in CML, S_1, S_2 and L layers and a transmission electron micrograph after $KMnO_4$ staining of phloem fibres in *M. japonicus* (Tree 5, b) showing cell wall structure of S_1+S_2+5 (G+L).

the degree of staining in the L_3 and G_3 layers was similar to that in the outer L_1, L_2, G_1 and G_2 layers (Figure 4c and d).

Immunolabelling of xylan

Figure 5 shows the results of immunolabelling with anti-xylan monoclonal antibody (LM10). The results from LM11 immunolabelling were very similar to LM10 labelling (data not shown). LM10 and LM11 recognize linear and low-substituted xylans from both mono- and dicotyledons, LM11 having greater affinity to substituted xylans (McCartney et al. 2005). LM10 labelling was found in the S_1, S_2 and L layers and almost no labelling was found in the G layers and CML (Figure 5b–d). Almost no labelling was found in the control, which did not contain primary antibody (data not shown). The labelling density was calculated from TEM micrographs of phloem fibres at different stages of development (Figure 6). Although it must be noted that these data were not obtained from the same phloem fibres, the change in labelling density provides information on the deposition process of xylan in various cell wall layers. The labelling density of the S_1 and S_2 layers did not significantly increase during the development of the multi-layered structure, suggesting that xylan deposition was almost completed by the time these layers were deposited. The labelling density of the L layers also did not significantly increase, suggesting that xylan deposition in these layers was also virtually completed by the time these layers were deposited and did not progress further until the next layer of cell wall was deposited.

Figure 7a and b shows the results of immunolabelling with anti-xylan monoclonal antibody (LM10) during the early stages of the L_2 layer formation. The developing thin L_2 layer showed no labelling with LM10, whereas the L_1, S_1 and S_2 layers were labelled, suggesting that xylan deposition in the L_2 layer did not occur during this stage. Almost no labelling was observed in control sections, which did not contain primary antibody (data not shown). Phloem fibres in the late stage of the L_3 layer formation are shown in Figure 7c and d. The innermost L_3 layer, with a greater thickness than the layer in Figure 7a and b, showed strong LM10 labelling (Figure 7c and d), suggesting that xylan deposition to the L_3 layer occurred during this stage.

Similar differences in xylan distribution between the thin early formed and thick fully developed L layers were found in the L_1, L_2 and L_3 layers.

Activity staining of peroxidase with metal-enhanced DAB

Figure 8 shows the results of peroxidase activity staining with metal-enhanced DAB by light microscopy. Peroxidase activity appears brownish colour in this technique. During S_2 layer formation, strong staining was found in CML including cell corners (arrows in Figure 8a) and S_1 and S_2 layers were weakly stained. When G layers are formed (Figure 8b), staining was found in developing G layers and activity in cell corner middle lamella and S_1, S_2 layers decreased. After thick G and L layers were formed (Figure 8c), very weak staining was found in G and L layers. No staining was found in control (Figure 8d).

The results of peroxidase activity staining with metal-enhanced DAB by transmission electron microscopy are shown in Figure 9. In this technique, peroxidase activity appears as precipitates of osmium owing to the high affinity of osmium to DAB. Because some osmium precipitates can be generated in the absence of DAB, peroxidase activity due to the presence of DAB was considered in comparison with a control with no addition of DAB. When compared with the control (Figure 9d and e), strong peroxidase activity was found in the thin L_3 layer in the early stages of formation and also in cytoplasm residues (Figure 9b), whereas almost no activity was found in fully developed L_1 and L_2 layers (Figure 8c). Although some precipitate was found in the G layers (both DAB-treated and control sections), the degree of staining of the G layers in the DAB-treated section was slightly higher than that in the control section, suggesting that there may be weak peroxidase activity in the G layers during the early stages of L layer formation.

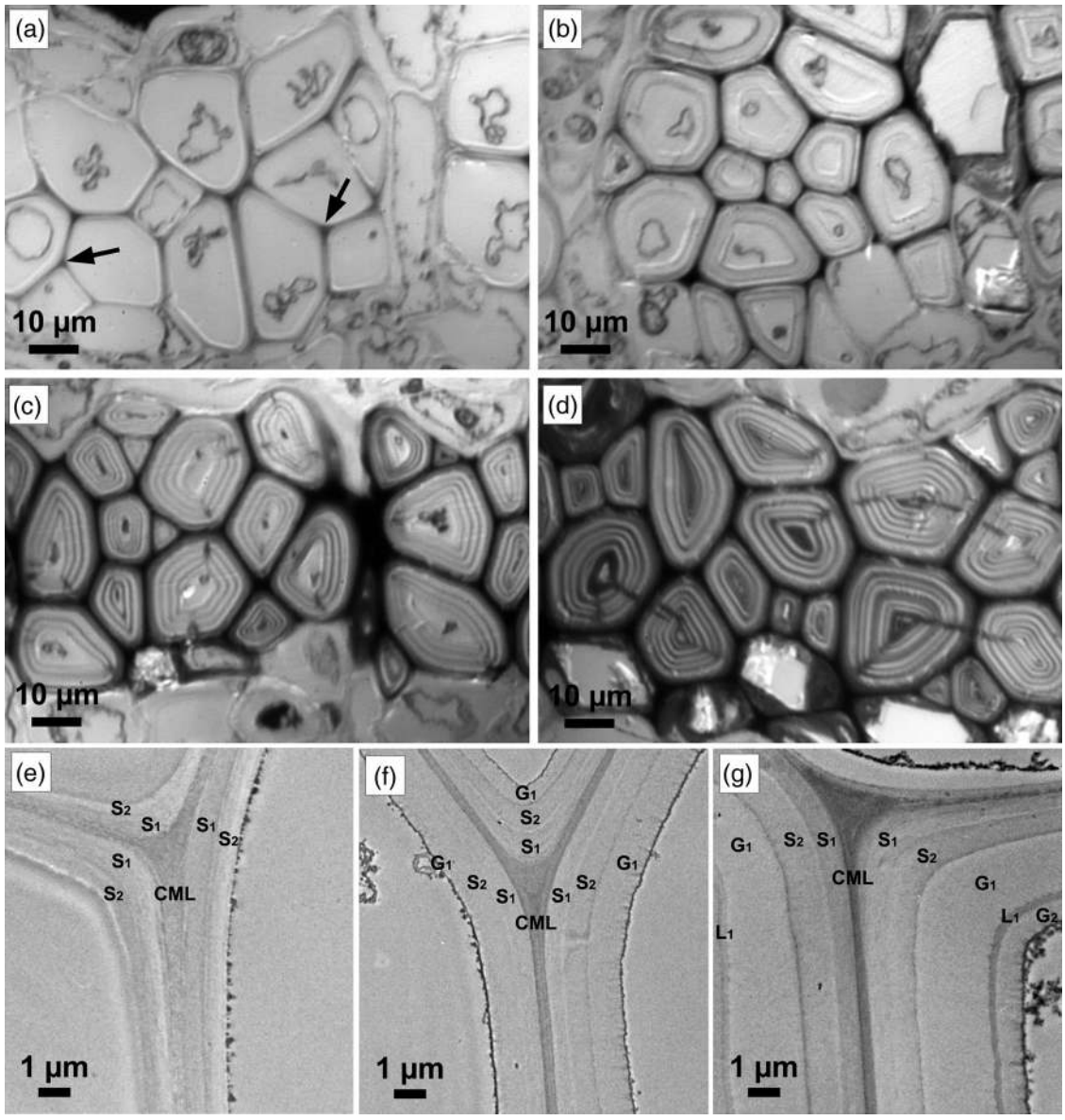

Figure 3. Ultraviolet micrographs taken at 280 nm of phloem fibres in *M. japonicus* collected on 16 June 2009 (Tree 3, a and b), 9 September 2009 (Tree 6, c) and 2 December 2009 (Tree 9, d) and transmission electron micrographs of transverse sections of phloem fibres in *M. japonicus* after $KMnO_4$ staining at the S_2 layer formation stage (e), G_1 layer formation stage (f), and L_1 (left) and G_2 (right) layer formation stages (g) showing the process of lignification.

In addition, no activity was found in the CML, S_1 and S_2 layers during the early stages of the L_3 layer formation (Figure 9c).

Discussion

Distribution and deposition process of glucuronoxylan

Immunolabelling of the LM10 antibody clearly indicated that xylan is located in lignified cell wall layers (S_1, S_2 and L layers) but not the CML (Figure 5). The virtually stable labelling density of the S_1, S_2 and L layers (Figure 6) suggests that xylan deposition to these layers occurs appositionally, i.e., xylan is deposited onto the lignified layers directly and not by a penetrative mechanism and deposition does not occur after the layers are fully deposited. Awano et al. (1998) reported the deposition process for xylan in the differentiating xylem of Japanese beech (*Fagus crenata* Blume) and found that xylan deposition occurred in a penetrative way during the formation of the S_1, S_2 and S_3 layers of wood fibres. The results in the present study suggest that the deposition process is quite different between wood fibres in the xylem and phloem fibres in the phloem, although there remains a possibility that xylan deposition progressed together with some structural change in the epitopes (e.g., structure of side chains and/or masking of lignin).

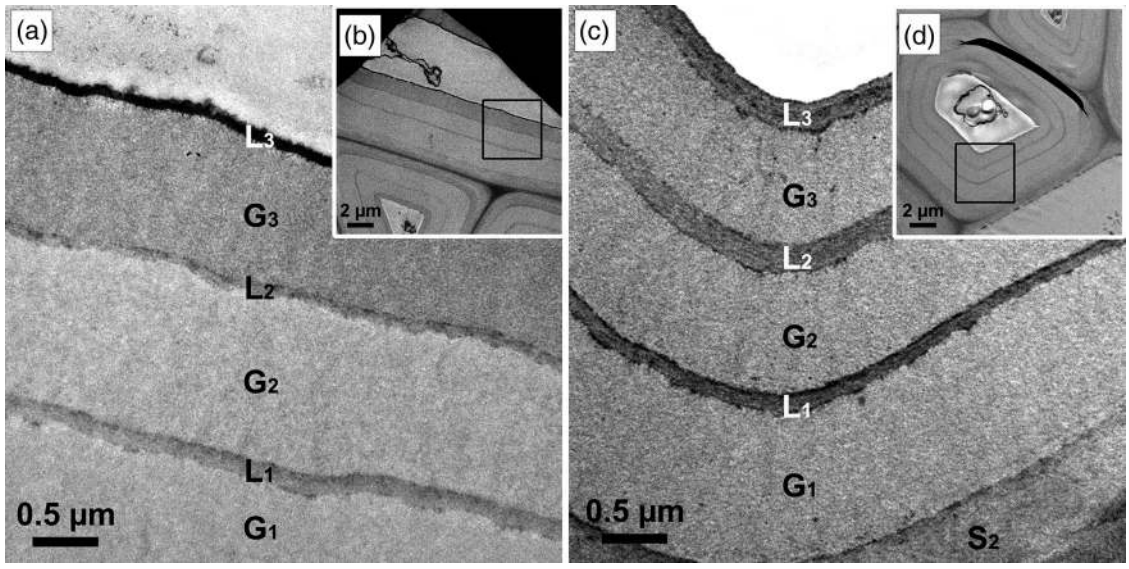

Figure 4. Transmission electron micrographs of transverse sections of phloem fibres in *M. japonicus* after $KMnO_4$ staining (Tree 5). (a and c) Enlarged images from the square regions shown in the smaller low-magnification images (b and d). (a and b) Phloem fibres in the early stages of L_3 layer formation. The L_3 layer was strongly stained. (c and d) Phloem fibres in the later stages of L_3 layer formation. The degree of staining of the L_3 layer was similar to that of the outer L_1 and L_2 layers.

Lignification process of S_1 and S_2 layers

Ultraviolet microscopy (Figure 3a–d) and potassium permanganate staining of the S_1 and S_2 layers (Figure 3e–g) clearly showed that lignification of the S_1 and S_2 layers progressed during G layer formation. This agrees with the result of a study on the lignification of lignified cell wall layers in poplar tension wood (Yoshinaga et al. 2012). If we assume that monolignols are synthesized within individual phloem fibres and transported to the lignifying cell wall layers as proposed for xylem cells by Wardrop (1971) and Samuels et al. (2002), our results suggest that monolignols must penetrate into and through the developing G layer during lignification of the S_1 and S_2 layers.

Another possibility is that living phloem and phloem ray parenchyma cells adjacent to phloem fibres may be involved in the lignification of phloem fibres located in the periphery of the fibre bundle, as hypothesized for tracheary elements based on a study in *Zinnia* (Hosokawa et al. 2001). Studies of the tissue-specific expression of enzymes related to lignin biosynthesis, such as caffeoyl coenzyme A *O*-methyltransferase (CCoAOMT, Zhong et al. 2000), cinnamyl alcohol dehydrogenase (Feuillet et al. 1995), phenylalanine ammonia-lyase (Bevan et al. 1989), 4-coumarate:coenzyme A ligase (Hauffe et al. 1991) and cinnamate 4-hydroxylase (Franke et al. 2000), have also suggested that ray parenchyma cells play some role in monolignol biosynthesis in the lignification of xylem cells. Some of these studies have also suggested a possible role of phloem and/or phloem ray parenchyma cells in lignification. Ros Barceló (2005) also suggested a role for xylem parenchyma cells during lignification. Recently, non-cell-autonomous postmortem lignification was suggested for tracheary elements in *Zinnia elegans* Jacq. (Pesquet et al. 2013). The contribution of neighbouring parenchyma cells to *Arabidopsis* xylem lignification and cell autonomous for lignification of the extra-xylary fibres was reported (Smith et al. 2013). It is unclear whether the two mechanisms (cell-autonomous lignification and the possible involvement of neighbouring phloem and/or phloem ray parenchyma cells) act together or one after the other. To determine which mechanism is operating, there is a need to evaluate the presence and distribution of monolignols or/and monolignol glucosides in phloem and/or ray parenchyma cells by Raman microscopy and matrix-assisted laser desorption/ionisation time-of-flight mass spectrometry, as described by Morikawa et al. (2010).

As described in the previous section, xylan deposition in the S_1 and S_2 layers might not occur after the layers are fully deposited, i.e., not in a penetrative way. Therefore, it can be assumed that lignification progresses in these layers when xylan is fully deposited. This may support the suggestion that xylan may act as a host structure for lignification (Reis and Vian 2004); however, more work will be necessary to prove the role of xylan in lignification. Because there was almost no xylan labelling in the CML, the other cell wall components, such as pectin, may have a close relationship with lignification in the CML.

Peroxidase activity was found in CML including cell corners and also S_1 and S_2 layers (Figure 8a). As lignification of CML, S_1 and S_2 layers progressed, the activity in these layers gradually decreased (Figure 8b and c). The presence of activity in these layers seems to be related to the lignification of CML, S_1 and S_2 layers. However, further work will be necessary to confirm that the activity is involved in lignification.

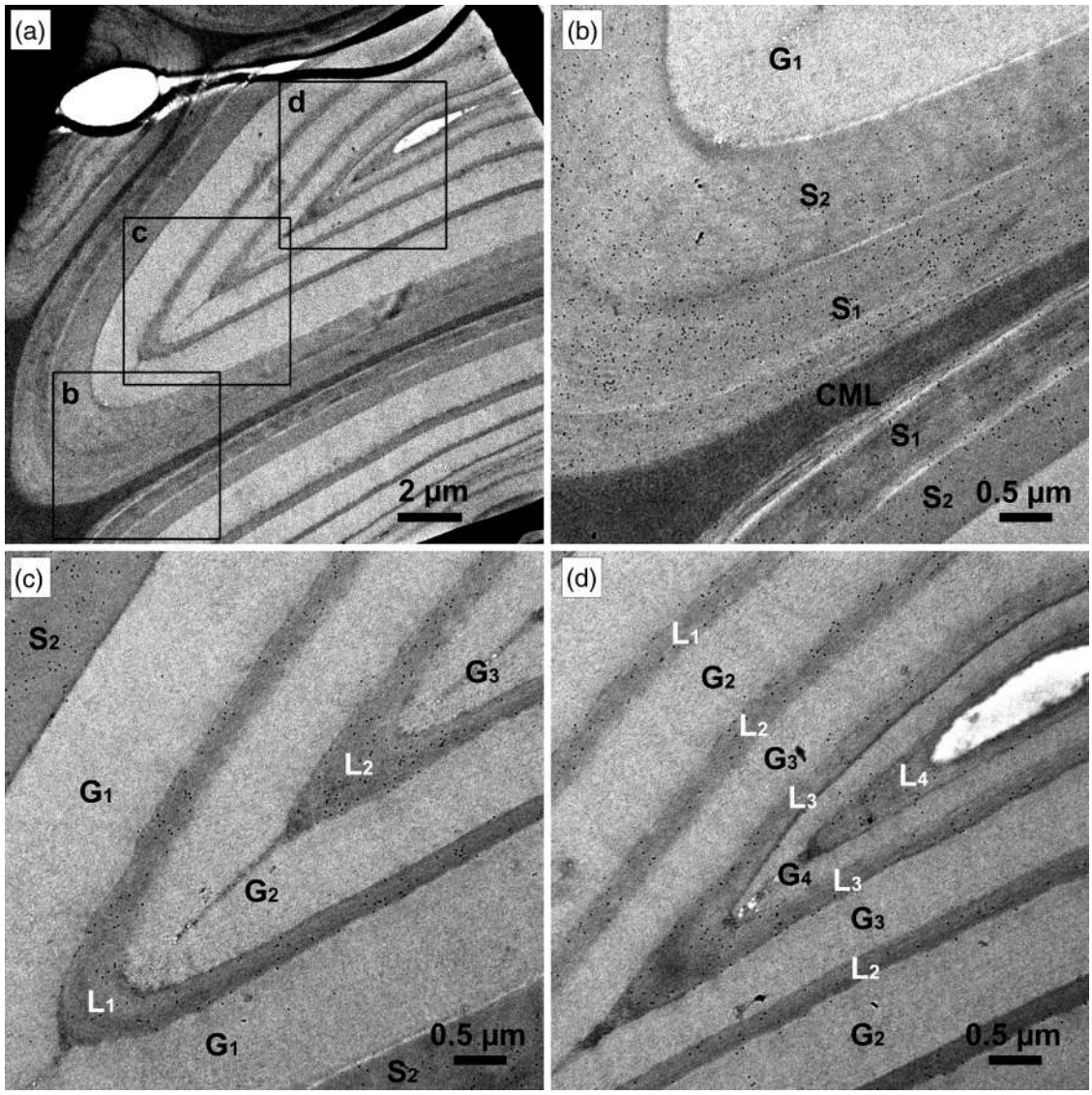

Figure 5. Immunolocalization of xylan in various cell wall layers in phloem fibres of *M. japonicus* (Tree 9) using LM10 antibody. (a) A low-magnification image showing one phloem fibre with multi-layered cell wall of S_1+S_2+4 (G+L). (b, c and d) Enlarged images from the square regions of the low-magnification image (a).

Peroxidase activity, xylan deposition and lignification process of the L layers

Activity staining with metal-enhanced DAB (Figure 9) showed strong activity in the L layers during the early stages of deposition. This result suggests that a part of a number of peroxidase isozymes should exist in the thin L layers during the early stages of deposition. In addition, these early L layers showed strong $KMnO_4$ staining (Figure 4) and no xylan labelling with LM10 (Figure 7a). The mechanism of $KMnO_4$ staining was discussed by Bland et al. (1971). They reported that the presence of phenolic hydroxyl groups in lignin was important for $KMnO_4$ staining. Therefore, the strong staining in the early L layers suggests that these layers may contain lignin rich in free phenolic hydroxyl groups that will undergo polymerization. Because some amino acids also display positive $KMnO_4$ staining, as reported by Bland et al. (1971), the presence of peroxidase or other proteins may also result in the strong staining of these layers. These results suggest that lignification had started with the presence of peroxidase, whereas xylan deposition had not yet started in the thin L layers that were being deposited. The role of peroxidase that was also found in the G layers, adjacent to the L layers that were being formed, was unclear. The presence of peroxidase in the G layer in tension wood was also reported by Wardrop and Scaife (1956). Further work is currently in progress to confirm whether peroxidase has the ability to polymerize monolignols or not.

In later stages of L layer formation, no peroxidase activity was found and the degree of staining with $KMnO_4$ decreased (Figure 4c), but strong xylan labelling with LM10 was found (Figure 7c). A decrease in the degree of $KMnO_4$ staining

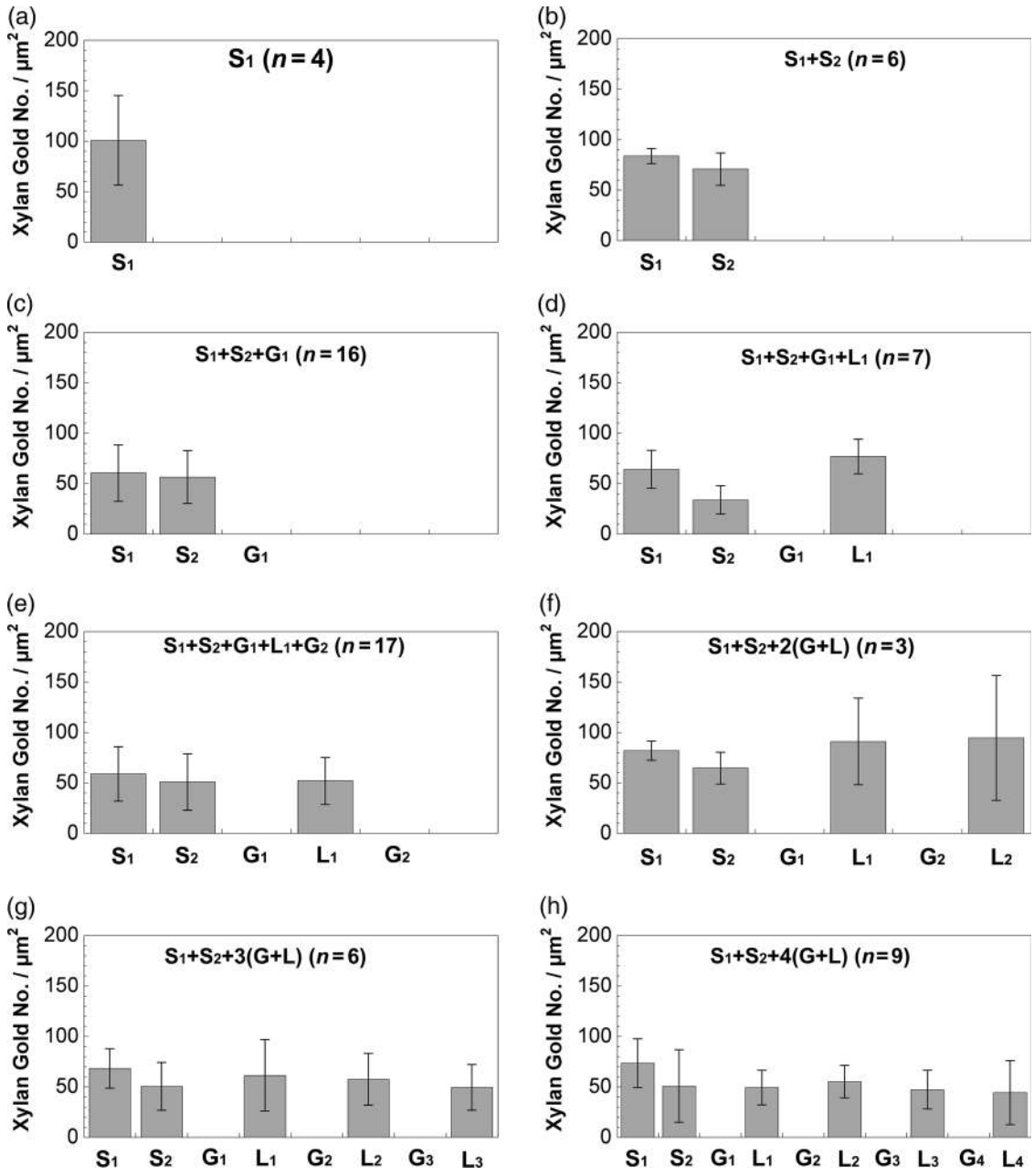

Figure 6. Quantification of xylan (LM10) labelling in various cell wall layers in phloem fibres of *M. japonicus* at the S_1 layer formation stage (a), S_2 layer formation stage (b), G_1 layer formation stage (c), L_1 layer formation stage (d), G_2 layer formation stage (e), L_2 layer formation stage (f), and in developed phloem fibres of the S_1+S_2+3 (G+L) type and (g) developed phloem fibres of the S_1+S_2+4 (G+L) type (h). *n*, cell numbers for quantification of labelling density. Error bars show the standard deviation.

suggests that lignification of the layers progressed with phenolic hydroxyl groups being consumed for the formation of interunit linkages. The presence of xylan labelling suggests that xylan deposition might have occurred on the polymerized lignin due to the activity of peroxidase during the early stages of L layer formation. This does not agree with the hypothesis of Reis and Vian (2004). On this point, however, further work will be necessary on the specificity of DAB staining and the role of enzymes existing in thin L layers.

Formation process of the multi-layered structure of phloem fibre cell walls

From the overall results of the present study, the formation process of the multi-layered structure of phloem fibre cell walls can be summarized as follows. During the formation of the S_1 and S_2 layers, xylan deposition progressed appositionally. During the formation of the G_1 layer, lignification of the CML, S_1 and S_2 layers progressed. After a thin L_1 layer was deposited, lignification occurred

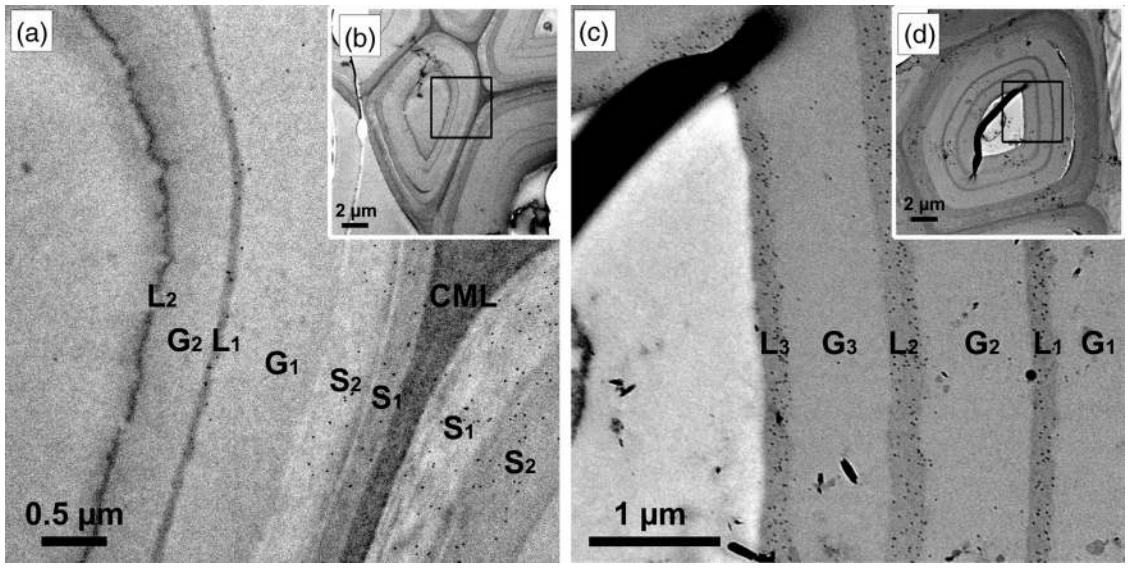

Figure 7. Immunolocalization of xylan in the phloem fibre of *M. japonicus* (Tree 5) in the early stage of L_2 layer formation (a and b) and in the later stage of L_3 layer formation (c and d). (a and c) are enlarged images from the square regions shown in the smaller low-magnification images (b and d). No immunolabelling of xylan (LM10 antibody) was found in the thin L_2 layer that formed early, while the outer L_1, S_1 and S_2 layers were labelled (a and b). Strong immunolabelling of xylan (LM10 antibody) was found in the developed L_1, L_2 and L_3 layers (c and d).

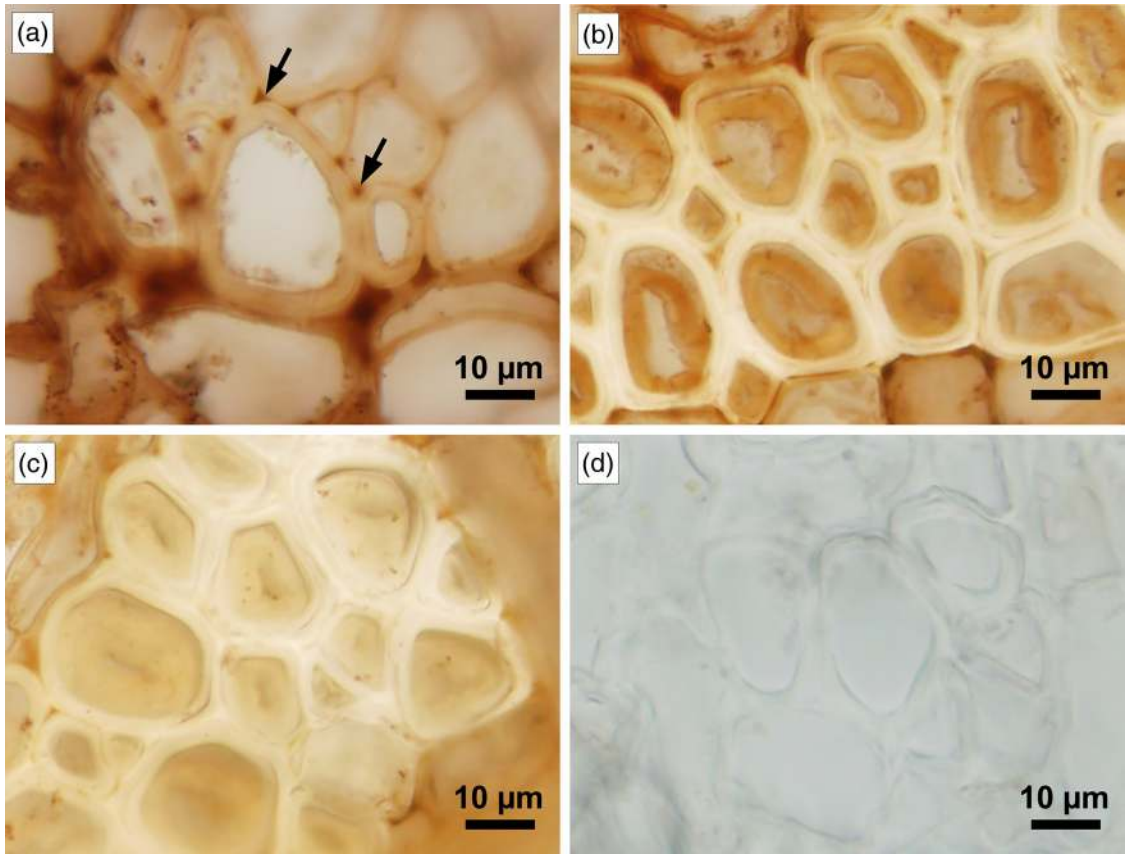

Figure 8. Light micrographs of transverse sections stained with DAB showing peroxidase activity of phloem fibres in *M. japonicus* (Trees 10 and 11) at the S_2 layer formation stage (a), during the development of G layers (b), and after the thick G and L layers are formed (c). (d) Control (omission of the DAB substrate) of phloem fibres at the S_2 layer formation stage. Strong activity was found in CML including cell corners (arrows) and weak activity was observed in S_1 and S_2 layers at the S_2 layer formation stage (a). The activity was then observed in developing G layers during G layer formation (b). Very weak activity was found in thick, developed G and L layers (c).

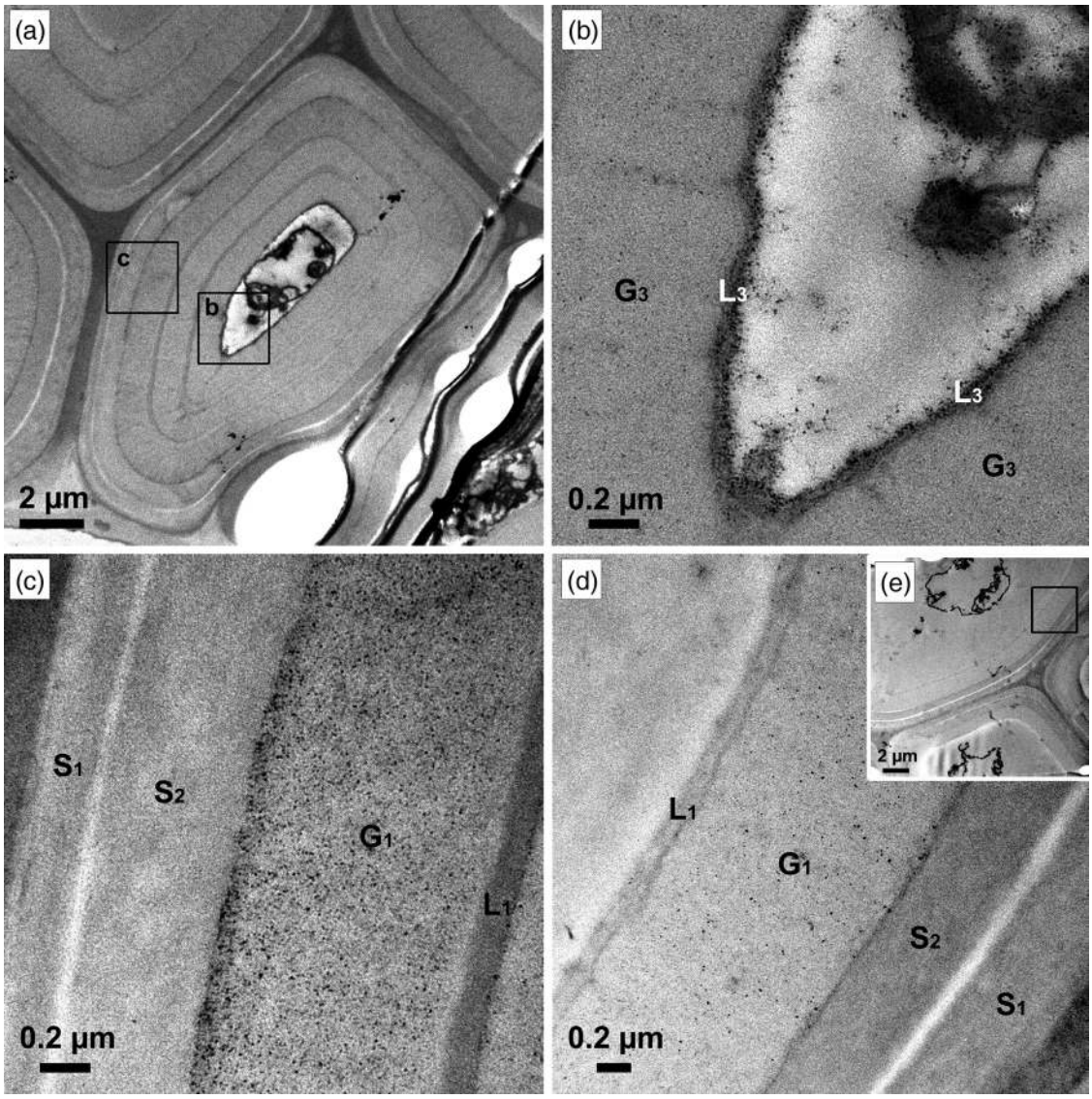

Figure 9. Transmission electron micrographs of transverse sections of phloem fibres of *M. japonicus* (Tree 4) after staining with DAB showing peroxidase activity as osmium (Os) precipitates. (a) A low-magnification image showing one phloem fibre in the early stages of L_3 layer formation. (b and c) Enlarged images from the square regions in (a). Peroxidase activity was found in the L_3 layer that formed early and also in cytoplasm residues (b). Weak peroxidase activity was found in the G_1 layer but no activity was found in the fully developed L_1 layer and the S_1 and S_2 layers (c). (d) Enlarged image from the square region in (e), which shows the control (no DAB treatment and fixed with OsO_4) in the early stages of the L_1 layer. Almost no precipitate was found in the thin L_1 layer that formed early, whereas small amounts of precipitate were found in the G_1 layer.

as evidenced by the presence of peroxidase activity in the L_1 layer. At this stage, xylan had not yet been deposited in the L_1 layer. As the formation of the L_1 layer progressed, lignification and xylan deposition progressed. Then the formation of the G and L layers occurred alternately to form the multi-layered cell wall structure. In the tension wood of *M. japonicus*, we found that tension wood fibres also have a peculiar multi-layered structure [$S_1+S_2+G+n(L+G)$; $n=2$, very thin lignified L layer] (Nakagawa et al. 2012). Further work is currently in progress regarding xylan deposition and lignification of these cell wall layers in tension wood fibres.

Conclusion

The present study clarified the process of xylan deposition and lignification in the S_1, S_2 layers and the L layers in the multi-layered cell walls of phloem fibres in *M. japonicus*. Further work will be necessary to clarify the role of peroxidase located in the CML, S_1 and S_2 layers during S_2 layer formation, in the thin L layers in early stages of deposition and also found in the innermost G layers.

Acknowledgments

The authors thank members of the Laboratory of Tree Cell Biology of Kyoto University for their kind support.

Conflict of interest

None declared.

References

Adams JC (1981) Heavy metal intensification of DAB-based HRP reaction product. J Histochem Cytochem 29:775.

Awano T, Takabe K, Fujita M (1998) Localization of glucuronoxylans in Japanese beech visualized by immunogold labelling. Protoplasma 202:213–222.

Bevan M, Shufflebottom D, Edwards K, Jefferson R, Schuch W (1989) Tissue- and cell-specific activity of a phenylalanine ammonia-lyase promoter in transgenic plants. EMBO J 8:1899–1906.

Bland DE, Foster RC, Logan AF (1971) The mechanism of permanganate and osmium tetroxide fixation and the distribution of lignin in the cell wall of *Pinus radiata*. Holzforschung 25:137–143.

Clair B, Ruelle J, Beauchêne J, Prévost MF, Fournier M (2006) Tension wood and opposite wood in 21 tropical rain forest species. 1. Occurrence and efficiency of the G-layer. IAWA J 27:329–338.

Feuillet C, Lauvergeat V, Deswarte C, Pilate G, Boudet AM, Grima-Pettenati J (1995) Tissue- and cell-specific expression of a cinnamyl alcohol dehydrogenase promoter in transgenic poplar plants. Plant Mol Biol 27:651–667.

Franke R, McMichael CM, Meyer K, Shirley AM, Cusumano JC, Chapple C (2000) Modified lignin in tobacco and poplar plants over-expressing the *Arabidopsis* gene encoding ferulate 5-hydroxylase. Plant J 22:223–234.

Graham RC, Karnovsky MJ (1966) The early stages of absorption of injected horseradish peroxidase in the proximal tubules of mouse kidney: ultrastructural cytochemistry by a new technique. J Histochem Cytochem 14:291–302.

Hauffe KD, Paszkowski U, Schulze-Lefert P, Hahlbrock K, Dangl JL, Douglas CJ (1991) A parsley 4CL-1 promoter fragment specifies complex expression patterns in transgenic tobacco. Plant Cell 3:435–443.

Hosokawa M, Suzuki S, Umezawa T, Sato Y (2001) Progress of lignification mediated by intercellular transportation of monolignols during tracheary element differentiation of isolated *Zinnia* mesophyll cells. Plant Cell Physiol 42:959–968.

Imagawa H, Ishida S (1973) Study on the development of secondary phloem in Harigiri (*Kalopanax pictus*). Bull Coll Exp For Hokkaido Univ 30:145–162.

Luft JH (1961) Improvements in epoxy resin embedding methods. J Biophys Biochem Cytol 9:409–414.

McCartney L, Marcus SE, Knox JP (2005) Monoclonal antibodies to plant cell wall xylans and arabinoxylans. J Histochem Cytochem 53:543–546.

Morikawa Y, Yoshinaga A, Kamitakahara H, Wada M, Takabe K (2010) Cellular distribution of coniferin in differentiating xylem of *Chamaecyparis obtusa* as revealed by Raman microscopy. Holzforschung 64:61–67.

Nakagawa K, Yoshinaga A, Takabe K (2012) Anatomy and lignin distribution in reaction phloem fibres of several Japanese hardwoods. Ann Bot 110:897–904.

Nanko H (1979) Studies on the development and cell wall structure of sclerenchymatous elements in the secondary phloem of woody dicotyledons and conifers. PhD Thesis, Kyoto University, Japan (in English).

Nanko H, Saiki H, Harada H (1974) Structure and development of the secondary phloem in *Populus euramericana* Guinier. Bull Kyoto Univ For 46:179–189.

Nanko H, Saiki H, Harada H (1977) Development and structure of the phloem fibres in the secondary phloem of *Populus euramericana*. Mokuzai Gakkaishi 23:267–272.

Nanko H, Saiki H, Harada H (1982) Structural modification of secondary phloem fibres in the reaction phloem of *Populus euramericana*. Mokuzai Gakkaishi 28:202–207.

Pesquet E, Zhang B, Gorzsás A (2013) Non-cell-autonomous postmortem lignification of tracheary elements in *Zinnia elegans*. Plant Cell 25:1314–1328.

Reis D, Vian B (2004) Helicoidal pattern in secondary cell walls and possible role of xylans in their construction. C R Biol 327: 785–790.

Richardson KC, Jarret L, Finke EH (1960) Embedding in epoxy resins ultrathin sectioning in electron microscopy. Stain Technol 35:313–316.

Ros Barceló A (2005) Xylem parenchyma cells deliver the H_2O_2 necessary for lignification in differentiating xylem vessels. Planta 220:747–756.

Ruelle J, Yoshida M, Clair B, Thibaut B (2007) Peculiar tension wood structure in *Laetia procera* (Poepp.) Eichl. (Flacourtiaceae). Trees 21:345–355.

Samuels AL, Rensing KH, Douglas CJ, Mansfield SD, Dharmawardhana DP, Ellis BE (2002) Cellular machinery of wood production: differentiation of secondary xylem in *Pinus contorta* var. *latifolia*. Planta 216:72–82.

Smith RA, Schuetz M, Roach M, Mansfield SD, Ellis B, Samuels L (2013) Neighboring parenchyma cells contribute to *Arabidopsis* xylem lignification, while lignification of interfascicular fibers is cell autonomous. Plant Cell 25:3988–3999.

Wardrop AB (1971) Occurrence and formation in plants. In: Sarkanen KV, Ludwig GH (eds) Lignins: occurrence, formation, structure and reactions. Wiley Interscience, New York, pp 19–41.

Wardrop AB, Scaife E (1956) Occurrence of peroxidase in tension wood of angiosperm. Nature 178:867.

Yoshinaga A, Kusumoto H, Laurans F, Pilate G, Takabe K (2012) Lignification in poplar tension wood lignified cell wall layers. Tree Physiol 32:1129–1136.

Zhong R, Herbert Morrison W III, Himmelsbach DS, Poole FL II, Ye Z-H (2000) Essential role of caffeoyl coenzyme A *O*-methyltransferase in lignin biosynthesis in woody poplar plants. Plant Physiol 124:563–577.